Aerothermal Protuberance Heating Design and Test Configurations for Ascent Vehicle Design

Charles E. Martin
United Space Alliance
NASA Marshall Space Flight Center

Richard D. Neumann
United Space Alliance – Geologics

Delma Freeman
NASA Langley Research Center

Aerothermal Protuberance Heating Design and Test Configurations for Ascent Vehicle Design

Charles E. Martin*, Richard D. Neumann, Delma Freeman
United Space Alliance & NASA Marshall Space Flight Center
MSFC, Alabama 35812
NASA Langley Research Center
Langley, Virginia
*Charles.e.martin@nasa.gov, Primary Author

Abstract

A series of tests were conducted to evaluate protuberance heating for the purposes of vehicle design and modification. These tests represent a state of the art approach to both testing and instrumentation for defining aerothermal protuberance effects on the protuberance and surrounding areas. The testing was performed with a number of wind tunnel entries beginning with the proof of concept "pathfinder" test in the Test Section 1 (TS1) tunnel in the Langley Unitary Plan Wind Tunnel (UPWT). The TS1 section (see Figures 1a and 1b) is a lower Mach number tunnel and the Test Section 2 (TS2) has overlapping and higher Mach number capability as showin in Figure 1c. The pathfinder concept was proven and testing proceeded for a series of protuberance tests using an existing splitter aluminum protuberance mounting plate, Macor protuberances, thin film gages, total temperature and pressure gages, Kulite pressure transducers, Infra-Red camera imaging, LASER velocimetry evaluations and the UPWT data collection system. A boundary layer rake was used to identify the boundary layer profile at the protuberance locations for testing and helped protuberance design. This paper discusses the techniques and instrumentation used during the protuberance heating tests performed in the UPWT in TS1 and TS2. Runs of the protuberances were made Mach numbers of 1.5, 2.16, 2.65, and 3.51. The data set generated from this testing is for ascent protuberance effects and is termed Protuberance Heating Ascent Data (PHAD) and this testing may be termed PHAD-1 to distinguish it from future testing of this type.

1. Introduction

Early in the space vehicle design process, adding external features, or protuberances, affected the thermal performance of the vehicle and its mission. In 1962 a series of tests were run in the UPWT to determine better what these effects were for a number of protuberance designs and parametric studies such as height and width. This data was compiled in the NASA Technical Note TN D-1372; "*Heat-Transfer and Pressure Measurements on a Flat-Plate Surface and Heat-Transfer Measurements on Attached Protuberances in a Supersonic Turbulent Boundary Layer at Mach Numbers of 2.65, 3.51, and 4.44*"; Paige B. Burbank, Robert A. Newlander, and Ida K. Collins, Langley Research Center. This data was used by the community for many years as the basis for initial protuberance design. Improvements in the acquisition technologies,

instrumentation, and materials used for the early protuberance testing have been dramatic and provide stark contrast to the inherent deficiencies in the TN-D 1372 report and data. Additionally, advances in Computational Fluid Dynamics (CFD) have allowed many design conditions to be modeled using computers rather than requiring the empirical developments of the past. All of these advancements allowed an evaluation of the effects of changes on the Space Shuttle configuration, especially for the local flow conditions around the protuberance. Vehicle changes required for the return to flight (RTF) effort of the Space Shuttle Program (SSP) amplified the need for better protuberance estimations and highlighted the current evaluation technique deficiencies. The relationships that are used to predict heating increases due to the addition of protuberances (or changes to protuberances) are termed bump factors. These bump factors are used to scale the undisturbed or "pre protuberance" heating by a scalar amount to account for heating on and around the protuberance. The bump factors are expressed in terms of the heating ratio of Hi (interference or protuberance heating) and Hu (undisturbed or no protuberance) typically expressed as Hi/Hu.
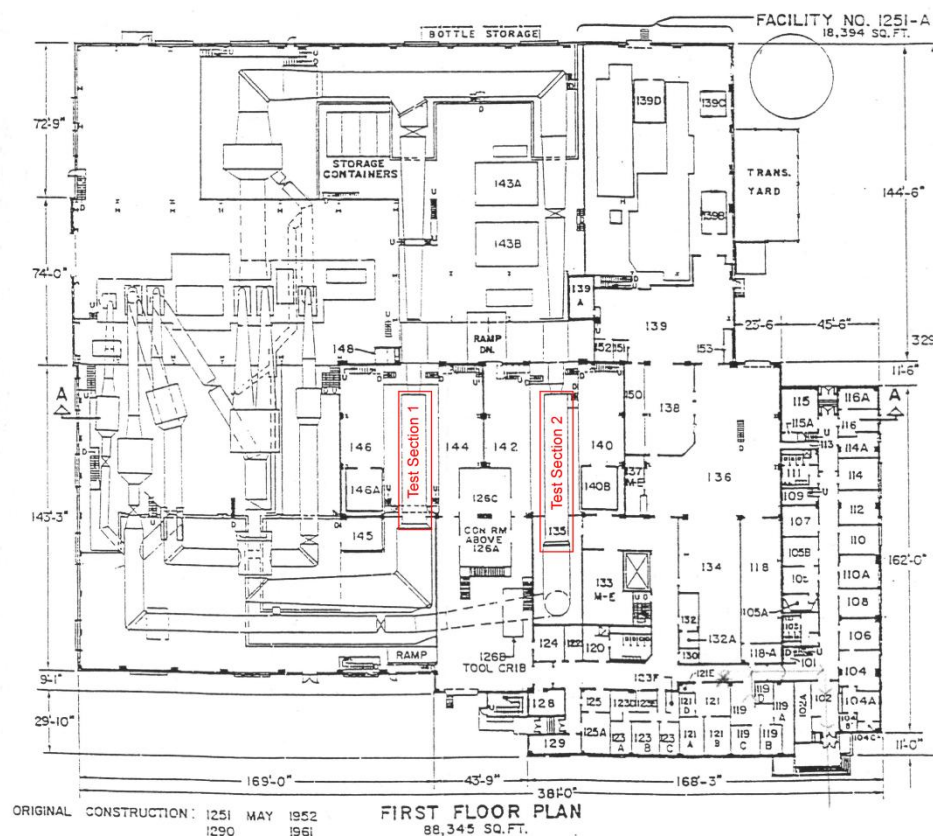

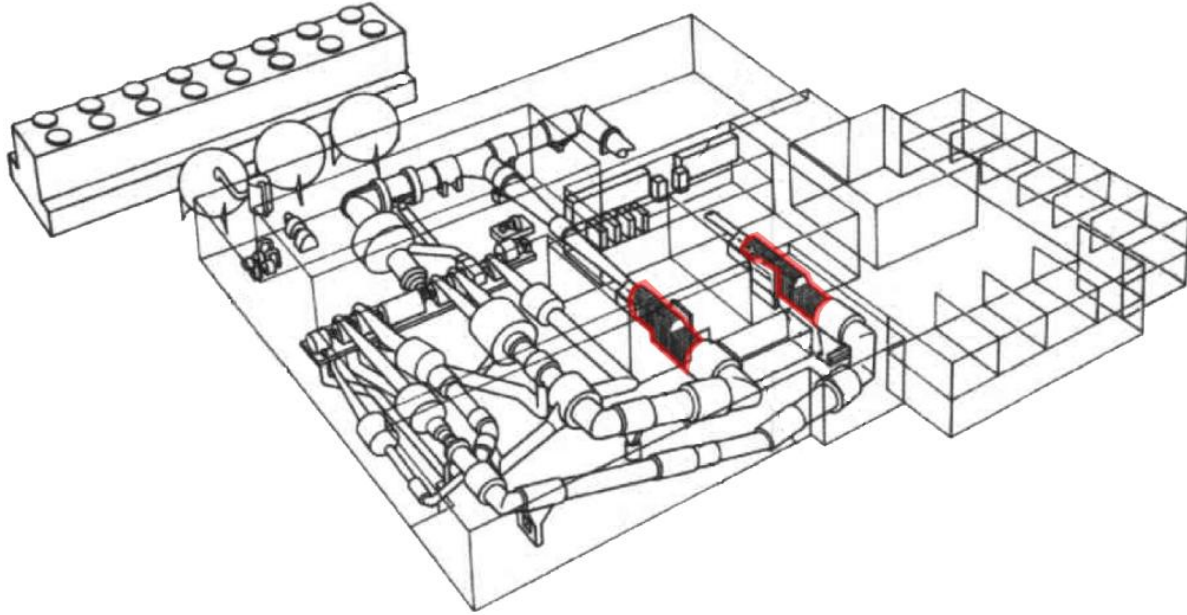Figure 1a. Langley Unitary Plan Wind Tunnel physical layout

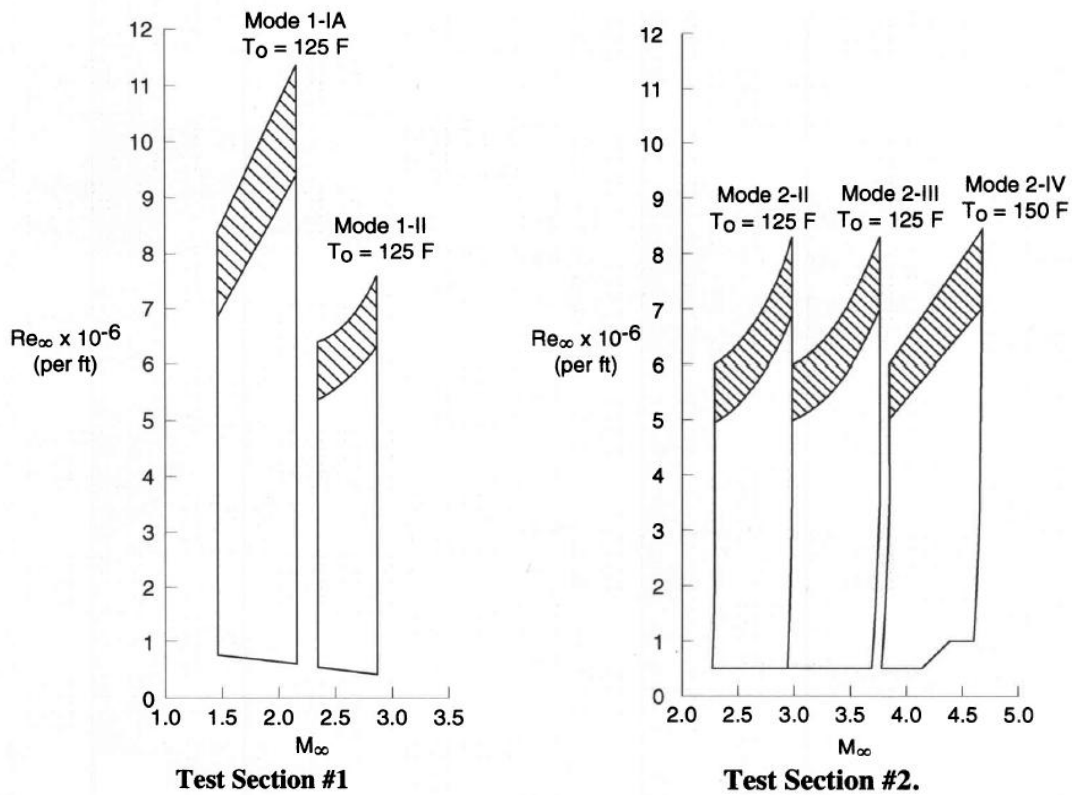Figure 1b. Langley Unitary Plan Wind Tunnel Showing Test Section 1 and 2

Figure 1c. Unitary Plan Test Section Mach Number and Reynold's Number Capabilities for Continuous Flow.

Figures 2 and 3 illustrate a generic protuberance and the effect of this protuberance on an undisturbed flat plate. Given the generic protuberance shape shown in Figure 2 and the affected flow area shown in red in Figure 3 illustrates the capability to predict the areas and levels of

heating influenced by protuberance addition can be difficult without some basis for estimation. This paper presents the testing configurations performed in the UPWT to address these issues.
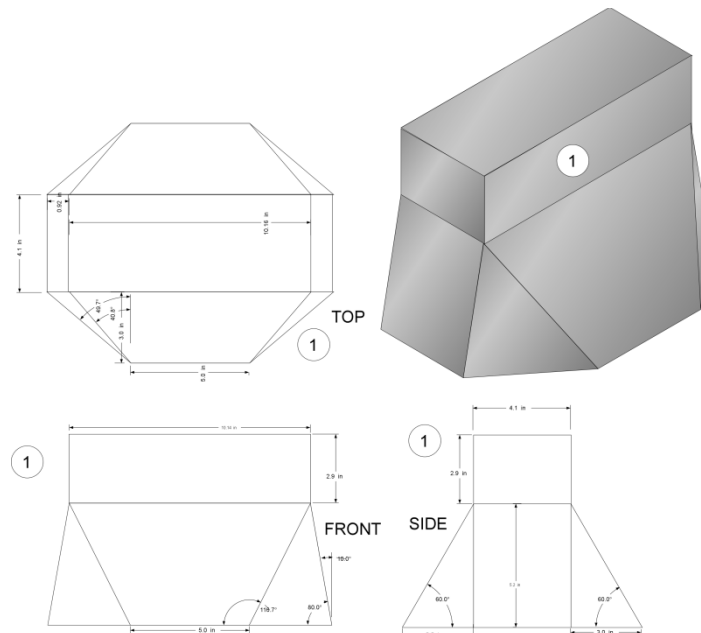

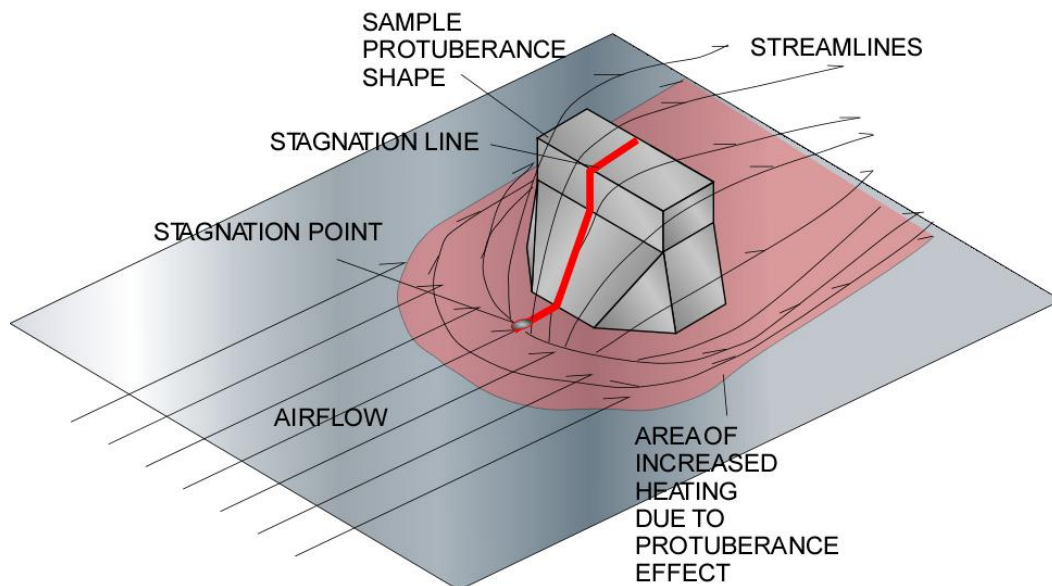Figure 2. Initial Generic Protuberance Shape Concept

Figure 3. Generic Protuberance Heating Effect.

2. Test Conditions

A new series of Wind Tunnel tests using state of the art technology was proposed to address protuberance heating for Mach Numbers 1.5, 2.16, 2.65 and 3.51 to determine heating and interference factors and to support future CFD heating analyses. These tests were designed to address the fact that Shuttle heating was initially developed for idealized geometries (smooth)

and then the protuberances were added. Flight scaling factors were developed following Orbital Flight Tests (OFT) to envelope differences between wind tunnel corrected data and OFT data The most recent methodology uses bump factors derived from the pressure ratio method (since pressure scales very well to heating) to adjust heating for changes in vehicle configuration and the resultant pressure changes due to design changes. However, this relationship is not as valid at lower Mach (tran-sonic) numbers and could be improved.

The overall purpose of this new testing was to enhance existing protuberance data with a set bump factors for use in vehicle development/modification and improve CFD heat factor/rate modeling capabilities.

Testing was performed in Test Section 1 (TS1) of the Unitary Plan Wind Tunnel (UPWT) located at Langley Research Center (refer to Figures 1a through 1c) for MACH Numbers 1.5 and 2.16 for a number of protuberances. LASER velocimetry for a clean plate, a 2.2 inch tall cylinder, and a 45/90 protuberance were run in TS1 to evaluate flowfield development. Testing in Test Section 2 (TS2) of the UPWT for MACH Numbers 2.65 and 3.51 was performed for the same protuberances. LASER velocimetry studies for MACH 2.65 and 3.51 for heat pulses with clean plate were performed in TS2.

The final goals of this test series were to correlate as run data for thin film, adiabatic wall measurement, and IR data to generate bump factors for protuberances and verify the results with select CFD runs and to Generate Parametrics on Aspect Ratio (width and height), wedge angles (30, 45, 75, 90), corner rounding, and cylinder (calibration cases).

3.   Instrumentation

To achieve the stated goals of the testing performed, several instrumentation improvements were made, including thin film sensors for temperature measurement, kulite pressure transducers for pressures, stagnation temperature gage with shroud for total temperature, etc.. Figure 4 shows the layout of the total temperature probe used to identify the freestream condtions of the flow in the tunnel during and after a heat pulse to determine the heat rate and changes to the protuberance due to air changes. Figure 5 shows the total pressure and total temperature gages on a support arm over the protuberance and splitter plate shown in Figure 6. The basis of the testing used to evaluate the protuberance effects was to run the tunnel at the specific Mach number until equilibrium was reached and then "pulsing" the tunnel by stopping cooling to the flow. This yielded a temperature rise of about 75 degrees F over a period of 10-15 seconds that allowed for the temperatures on the protuberance and surrounding areas to be measured using thin film gages. (see Figure 7). This pulse allows for heat transfer to be measured and the "response" of the protuberance and acreage to changes in heat potential. The constant flow UPWT facility did not allow for an "injection" of the splitter plate into the flow field to provide the greatest driving potential, which would have been the ideal testing case. Instead, the equilibrated model was affected by the warmer air pulse and it's response was measured. This

technique allows for errors in conduction and prevents a true equilibrium (or conduction free) condition to exist in the system prior to data measurement.
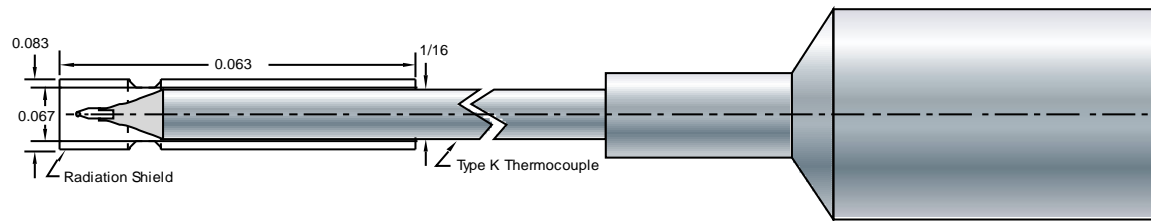

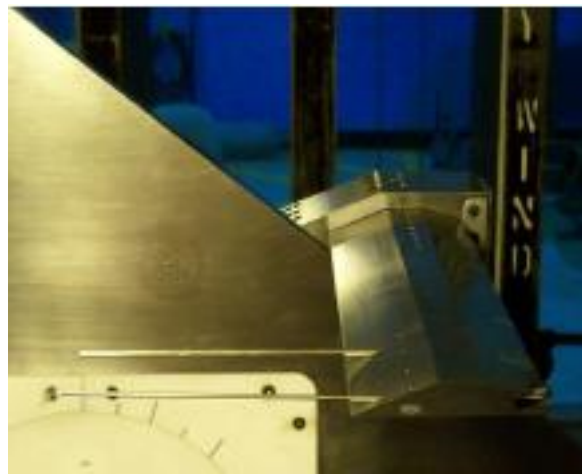Figure 4. Total Temperature Probe with Static with Tip Shield for Static Temperature Measurement

Figure 5. Location and design of Total Temperature and Total Pressure Probe above Splitter Plate
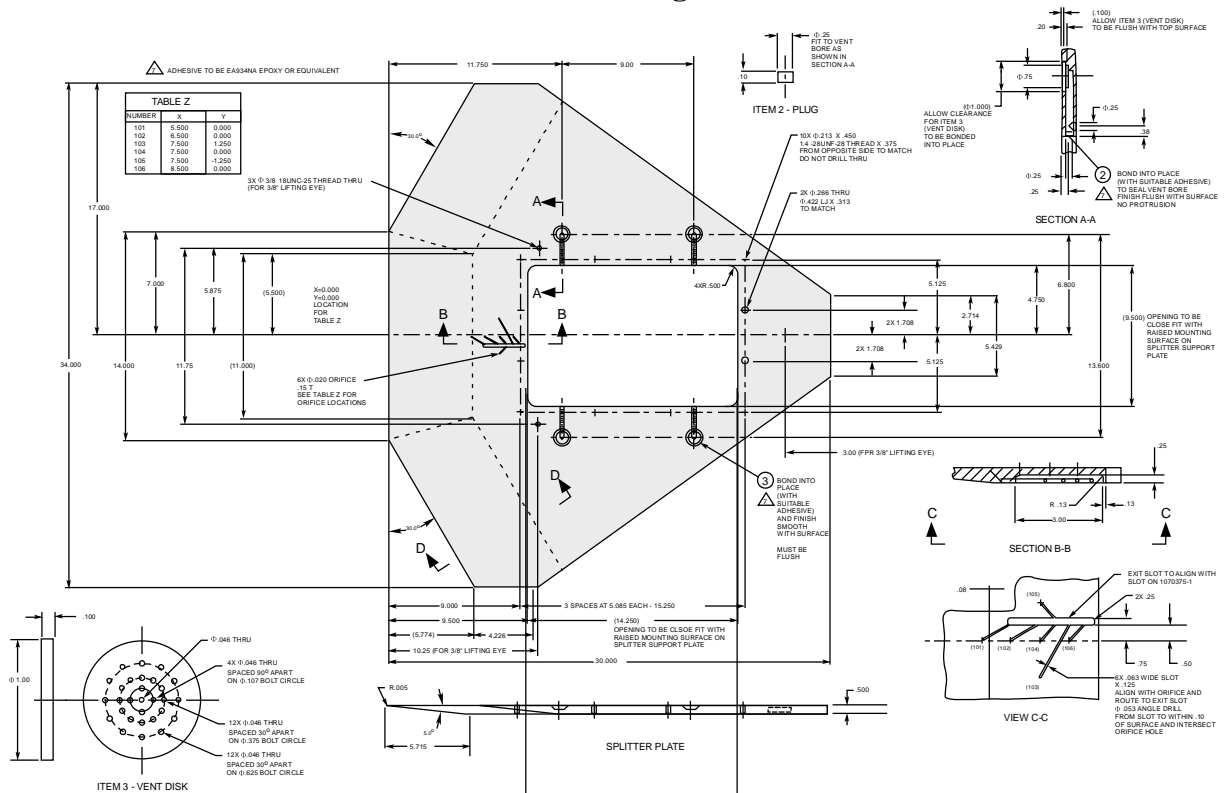
4. Hardware configurations

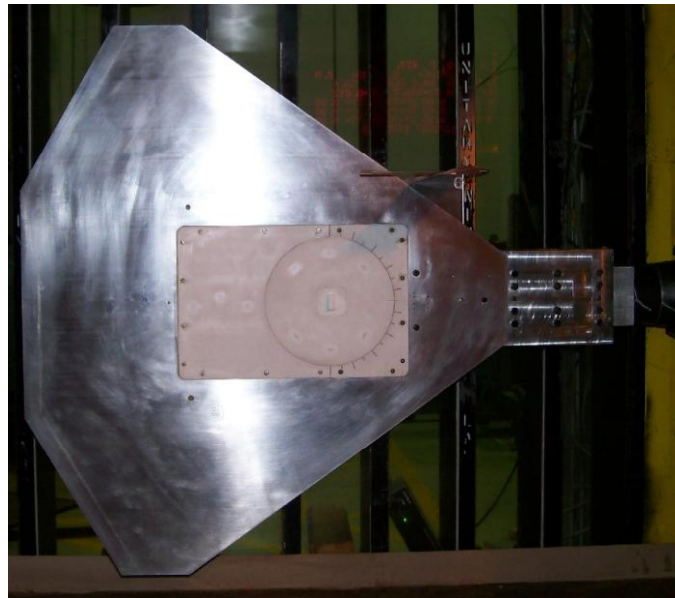Figure 6a. Aluminum Splitter Plate used in Protuberance Testing.

Figure 6b. Splitter Plate showing Macor insert, turntable, and Protuberance in Test Section 1.

The heart of the testing is the selection of the MACOR material (a white ceramic with low heat conductivity) and the thin film gage technology. Macor was machined, drilled, and heat treated for use in the testing and then platinum thin film serpentine gages were installed in the desired locations. Figure 7 illustrates the formation process and final dimensions of a typical thin film

gage. The contact wires were potted to the deposited platinum using conductive epoxy and the serpentine path was nominally perpendicular to the flow path to provide the most thermal response to the heated flow and therefore the most resistance to the induced electrical current to measure resistance change as a function of temperature. Each protuberance model with thin film gages were calibrated in an oil bath and calibration curves for each sensor were generated over the temperature ranges experienced during testing. Units in Figure 7 are inches.

Figure 7. Thin Film Gage Layout and Design.

Figures 8a and 8b illustrate the tunnel test section with the test hardware in place and the overall tunnel configuration. The protuberance height is exaggerated for clarity.
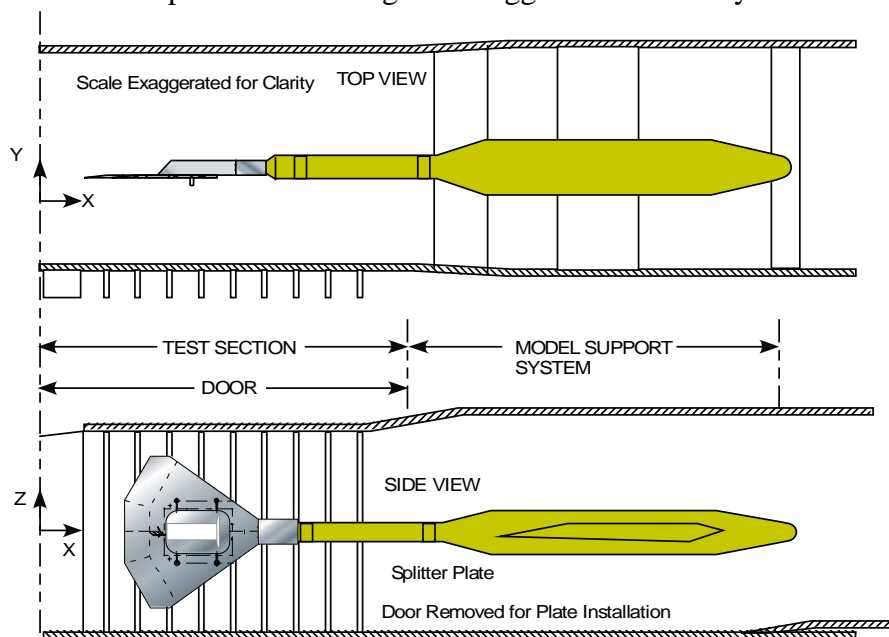

Figure 8a. Tunnel Section with Splitter Plate (for both Test Section 1 and 2)

Figure 8b. Unitary Plan Wind Tunnel Test Section and Throat.

The Splitter plate with a tested protuberance is shown in Figure 9 with the boundary layer estimation where the flow is from left to right. Many of the protuberances were protruding into the freestream slightly and therefore the top gages were exposed to the most extreme conditions while the gages embedded in the boundary layer provided data for the protuberance and surrounding acreage effects. Figure 10 shows the boundary layer "rake" used to determine the height and shape of the boundary layer experienced by the splitter plate and protuberance during the flow conditions generated by the tunnel.

Figure 9. Protuberance mounted in Splitter plate Showing Boundary Layer Height.
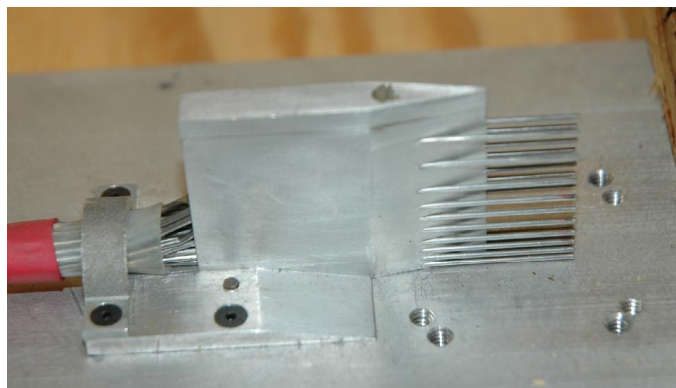

Figure 10. Boundary Layer Rake for evaluating Boundary Layer on Splitter Plate during Tunnel Flow

Part of the testing requirement was to determine the pressures at the temperature measurement locations for a handful of the primary protuberances. Figure 11 shows the piezoelectric pressure measurement gage made by Kulite. These gages were installed in four protuberances and corresponded to the locations where temperature measurements were made with thin film gages. Figures 12 and 13 illustrate the Macor protuberance with thin film gages and the aluminum pressure protuberance, respectively. Each hole in the aluminum protuberance was connected to a Kulite with a pressure tube to measure the instantaneous pressure response of the protuberance. This configuration clearly required duplicate runs for thermal and pressure data acquisition to form a complete data set. Each run had an accompanying heat pulse regardless of the instrumentation used.
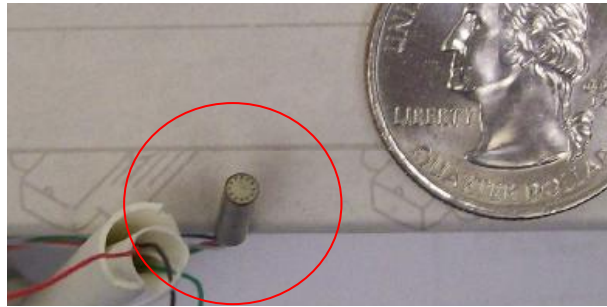

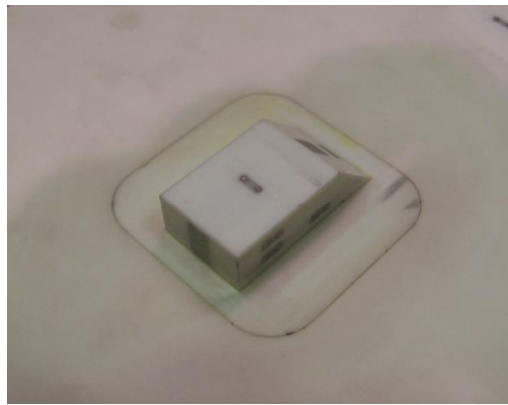Figure 11. Kulite Pressure Measurement Transducer

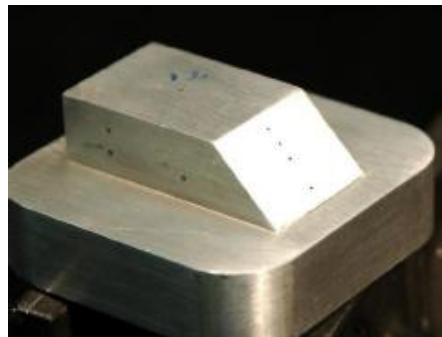Figure 12. Macor Protuerance Used in Protuberance Testing

Figure 13. Aluminum Pressure measurement Protuberance Matching Macor Protuberance.

In an effort to address protuberance and acreage heating effects due to alpha and beta (angle of attack or pitch angle and yaw angle) for flight, the capability to rotate the protuberance during testing was accomplished by mounting the protuberances in a rotating turntable and controlling the rate and amount of rotation with direct current (DC) stepper motors. Figure 14a shows the Macor turntable with thin film gages to measure rotation effects on the acreage. Figure 14b shows the layout of the instrumented Macor plate inserted into the splitter plate and shows the nominal start position for the system prior to heat pulsing.

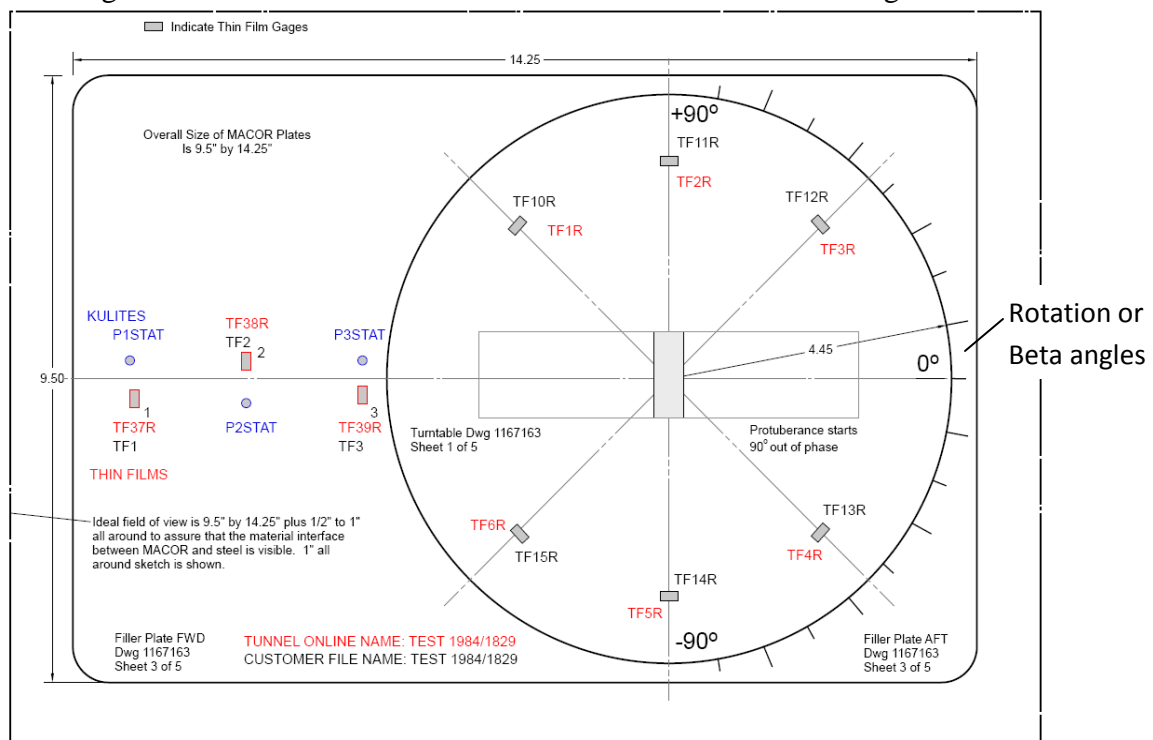Figure 14a. Macor Turntable insert with Protuberance Mounting Hole

Figure 14b. Macor insert, Turntable, and Protuberance Insert Showing Instrumentation and Dimensions

Due to the fact that the surrounding acreage near the protuberance is affected asymmetrically and since the number of gages that could be applied to the surface was both expensive and finite, Infra-Red (IR) thermography allowed for unprecedented data acquisition of the protuberance and surrounding acreage. It should be noted that only the surfaces perpendicular to the IR camera focal plane were measurable due to emissivity calibrations, therefore, any surfaces angled away from normal did not give true measurements and were not used. Using the IR thermography, it was a simple matter to determine a point far removed from the protuberance and use that data value as the undisturbed heating parameter (HU), and all other areas affected by the protuberance (Hi) values would be ratioed to that value to give the desired "bump factors". Figure 15 shows a typical IR screen image and Figures 16 and 17 show the reduced Tecplot data time samples used to generate the temperature/heat transfer coefficient ratios for different protuberances.
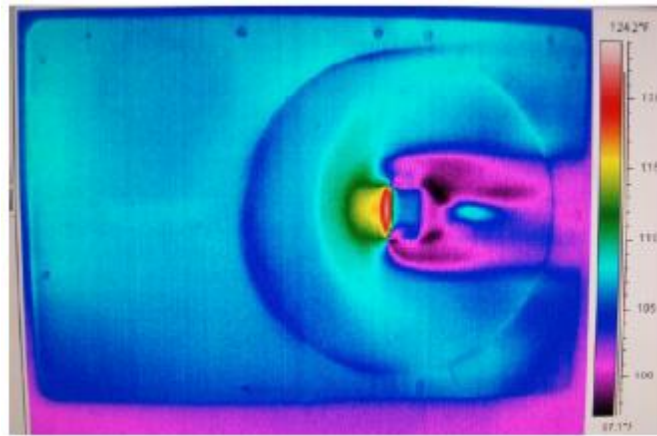

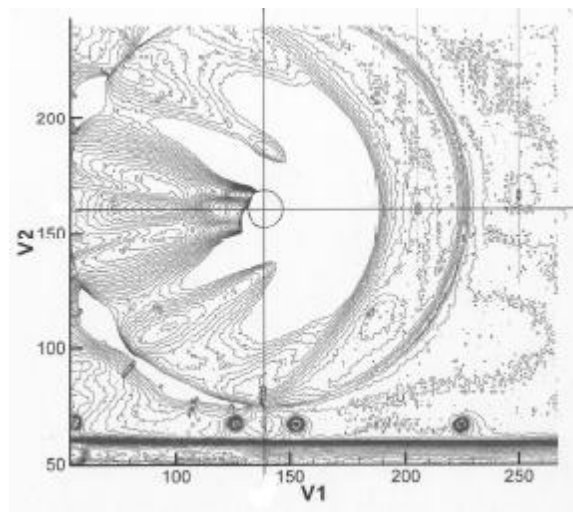Figure 15. Typical Infra Red Image of Macor Insert, Turntable, and Protuberance.

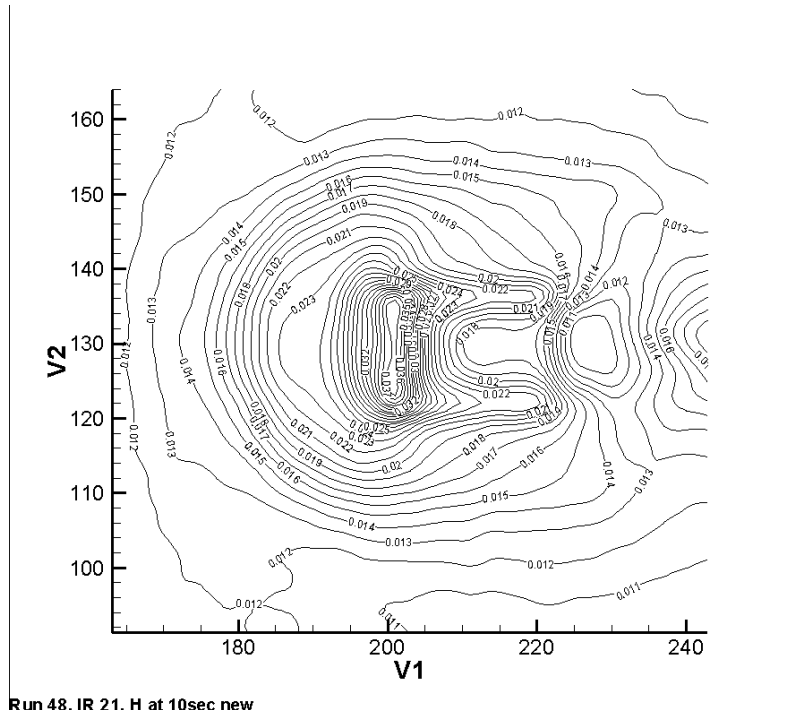Figure 16. Isotherms of data Reduced from IR Imagery.

Figure 17. Protuberance heat transfer coefficient (isotherms) during heat pulse for a 45 degree ramp face protuberance.

For Figures 15 and 17, the flow is from left to right, for Figure 16 the flow is from right to left. The heat pulse generated in the tunnel that made data measurement possible is shown in Figure 18.
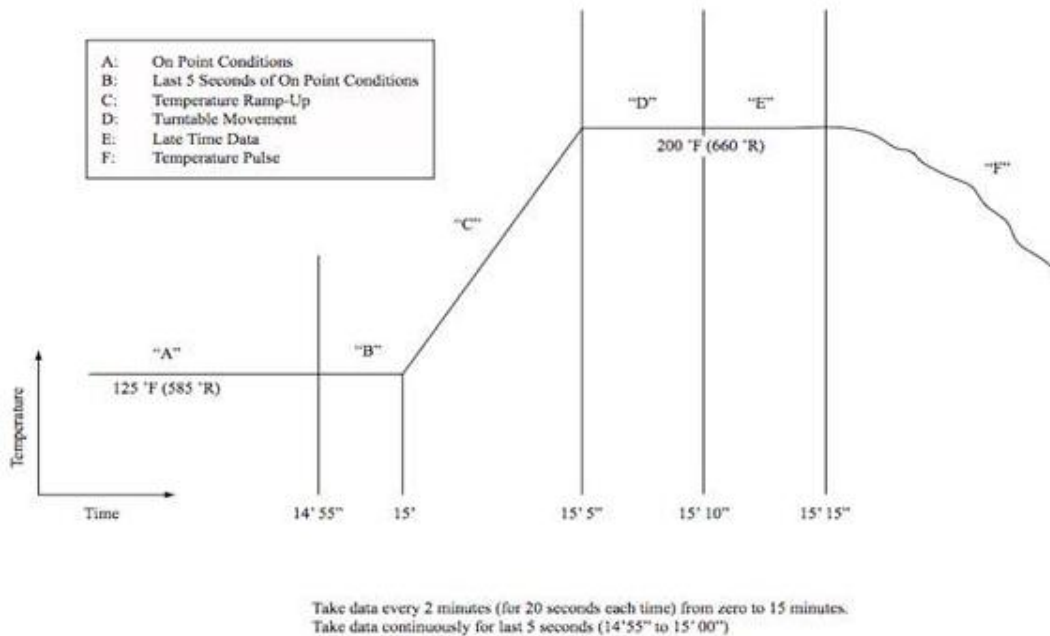

Figure 18. Temperature/Heat pulse Profile induced For Protuberance Runs.

Part of the primary parametrics run during testing, independent of specific protuberance shape, were width and height effects. Figure 19a and 19b show the same protuberance design, the first being 0.75 inches wide and the second being 5 inches wide. Both protuberances had identical instrumentation on their ends and the wider protuberance had instrumentation down the centerline where the stagnation point was expected to occur during primary run conditions. This provided data for end effects and centerline effects for differences in radial position of protuberance ends.
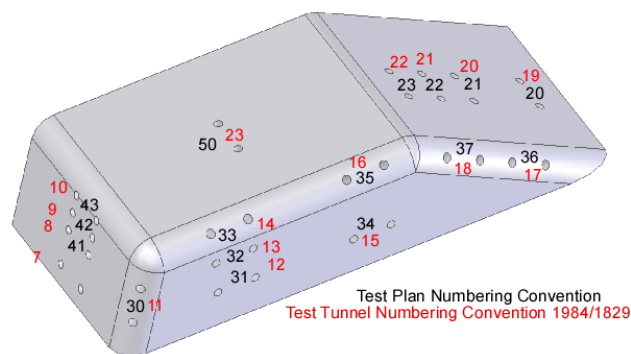

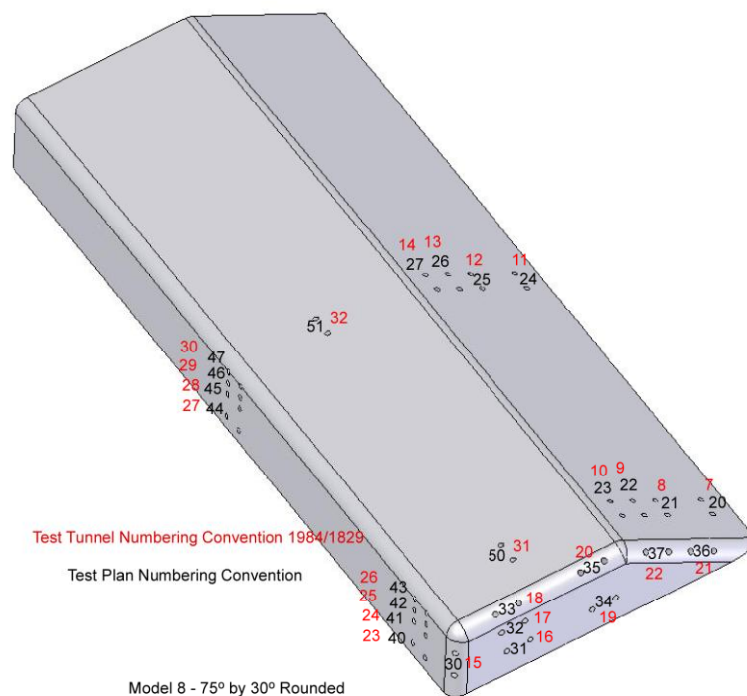Figure 19a. Narrow Protuberance Showing Instrumentation Location.

Figure 19b. Wide Protuberance Showing Instrumentation Location
Similarly,

Figure 20 shows tall and short cylinders, the short one being 0.4 inches tall, 0.75 inches in diameter and the tall one being same diameter but 2.2 inches tall. These were instrumented identically up to the 0.4 inch mark and provided the boundary layer heating for protuberances that extended into the freestream and just reached the height of the freestream. In keeping with the height parametric, a series of runs were made for protuberances 0.1, 0.2, 0.3 and 0.4 inches

tall, each having identical instrumentation locations from their bottom plane and each being instrumented the same on the sides and top to provide data on heating when a protuberance is completely immersed in the boundary layer. Figures 21a and 21b illustrate the protuberance shapes utilized to demonstrate the dual effects of height and width parameters evaluated for sharp edged protuberances.
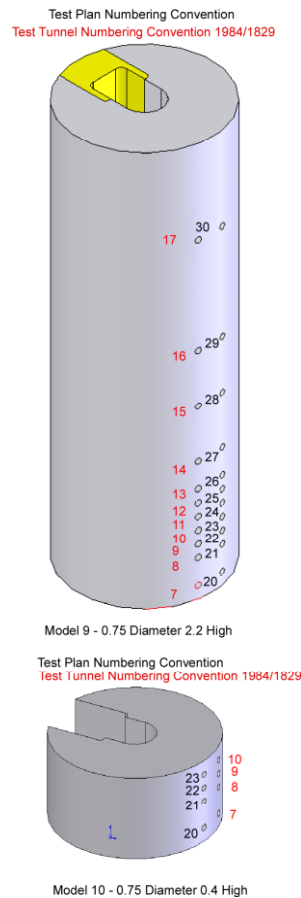

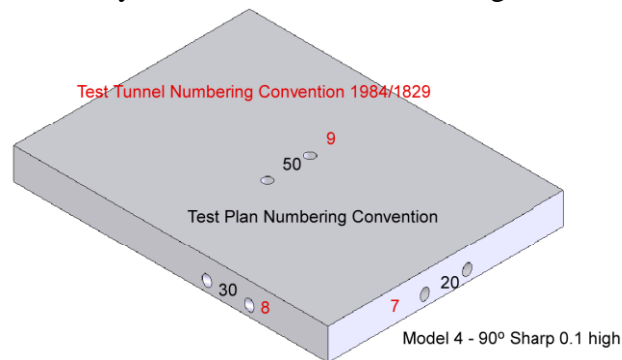Figure 20. Short and Tall Cylinder Protuberance Showing Instrumentation Locations.

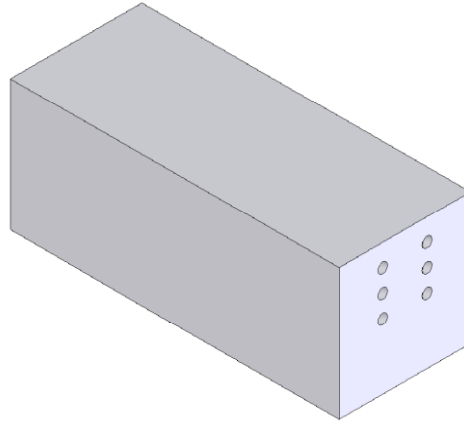Figure 21a. Short Sharp Protuberance

Figure 21b. Narrow Protuberance

Since there was no way to passively measure pressures on and ahead of the protuberance similar to the IR technique, a series of runs were made to measure the pressures, and therefore separation region, ahead of the square 0.3 inch high protuberance to compare to the CFD predictions for pressure ahead of this protuberance as a calibration point. Figure 22 illustrates the shape tested as well as the location of the pressure taps used for this measurement.
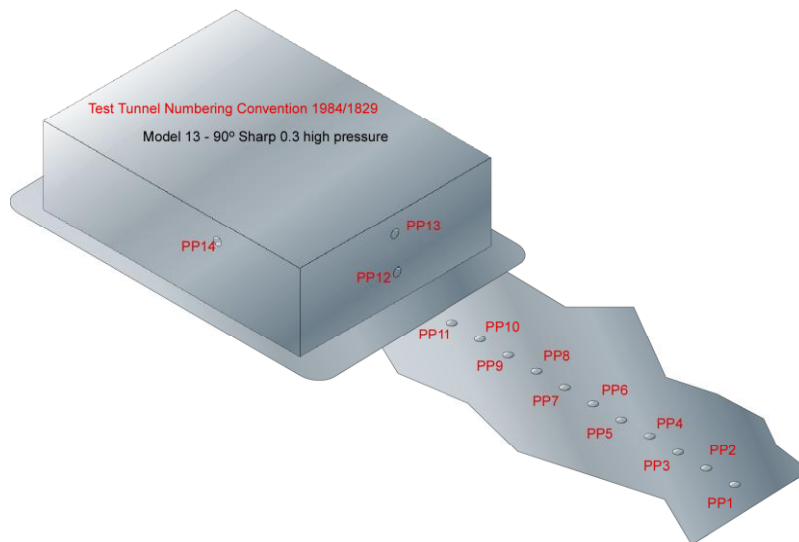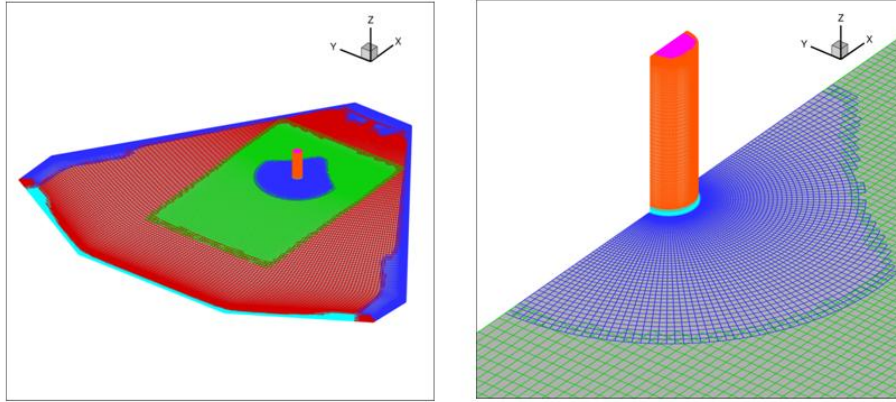

Figure 22. Pressure Measurement Protuberance evaluating Separation Region.

The final facet of the testing performed was the evaluation of CFD modeling to predict the testing outcomes using the given tunnel conditions and material properties. Several evaluations were made using the OVERFLOW code and the specific tunnel geometries. A sample of the grid mesh and description of the CFD approach are shown in Figure 21. The CFD final conclusions and results are still pending at this time and will be documented elsewhere.

5.   Analyses

- **CFD simulations were performed to determine the analytical results and experimental results differences. OVERFLOW code was used.**

- **Heat transfer coefficients computed using two CFD solutions:**
  - **Necessary to obtain both adiabatic wall temperature (T_{aw}) and heat flux (q")**
  - **Method of defining wall temperature for heat flux computation was found to cause some spurious results**

Figure 21. CFD evaluations of Tall Cylinder and stated goals of CFD analyses

Although great care was taken to design a system that minimized the conduction losses in the thin film instrumentation, it was determined that some conduction losses did occur and further evaluations were made to determine the level of conduction losses that were incurred. It should be noted that earlier protuberance testing (during early phases of space flight) used less responsive instrumentation and would have had significant conductive losses that the technology was simply unable to address at that time. Computational heat transfer analyses were performed by the University of Alabama for the project and were able to quantify the conductive losses experienced in a relatively timely manner. Improvements in modeling and greater results fidelity will be possible in the future and the initial heat conduction results show promising capability to evaluate wind tunnel induced conditions on protuberances and instrumentation given accurate temperature measurements during tunnel runs. Figure 22 shows a time step solution for the short cylinder during an inverse heat conduction solution run.
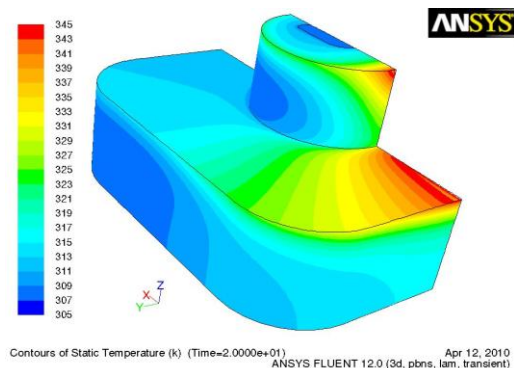

Figure 22. Heat Conduction Simulation Run Image.

6.   Summary

The testing described herein has been completed, the post test reports have been written but the final CFD and Data Reduction reports are still in work and are scheduled to be released later this year. Preliminary results indicate that the protuberance effects for local flow Mach number conditions are higher than previously expected but appear to be very well behaved when evaluated over the proper parametric indices. Additional testing in shock/blowdown tunnels and conductive evaluations are anticipated as part of the final application data manual that will allow the data set to be applied to a wide range of protuberance and ascent data designs.